

# Severe Complications Following Maxillary Sinus Augmentation Using Poly L-lactide-co-ε-caprolactone-Coated Bovine Bone: A Retrospective Study

Anat Ben-Dor, DMD<sup>1</sup>/Eran Gabay, DMD, PhD<sup>2</sup>/Jacob Horwitz, DMD<sup>2</sup>/  
Hadar Zigdon-Giladi, DMD, PhD<sup>2</sup>/Eli E. Machtei, DMD<sup>2</sup>/Yaniv Mayer, DMD<sup>1</sup>

**Purpose:** To describe the postoperative complications following lateral wall sinus augmentation using (poly L-lactide-co-ε-caprolactone; PLCL) and natural polysaccharides polymers-coated bovine bone (PBB). The secondary aims were to examine histologic findings and to propose complication management alternatives. **Materials and Methods:** This retrospective study included 61 subjects who underwent 67 lateral wall sinus augmentation procedures using PBB in the standard protocol. In cases that presented complications, treatment included additional antibiotic therapy, implant removal, or sinus reentry and total removal of the grafting material. In three cases, biopsy specimens were taken from the sinuses, and histologic analyses were performed. **Results:** The prevalence of postoperative complications was 32.8% (22 of 67 cases) in 18 of the patients (29.5%). The most prevalent symptoms were persistent pain (68.2%), swelling (63.6%), and oroantral fistula (54.5%). Radiographic signs appeared in 45.5% of the complications. A total of 24 implants failed; thus, an overall 80.3% survival rate was established at 19 months. The vast majority of complications (86.4%) were treated eventually with reentry surgery and revealed that the sinus was full with granulation tissue surrounding pieces of a nonossified rubber-like material. In cases where implants were placed, nonosseointegrated implants were surrounded by soft tissue. The sinus was cleaned thoroughly; the graft material remnants were removed together with inflamed parts of the sinus membrane, followed by chlorhexidine and saline lavages. In the biopsy specimens taken from the sinus cavity, there were no histologic features of new bone formation around the grafted material. **Conclusion:** Lateral wall maxillary sinus augmentation using PBB was associated with an acute sinus infection histologic appearance and with a 7-times-higher failure rate compared with previous reports. This serious adverse event suggests that PBB cannot be recommended for maxillary sinus augmentations. *Int J Oral Maxillofac Implants* 2021;36:1024–1031. doi: 10.11607/jomi.8792

**Keywords:** complication, implant failure, infection, graft failure, PLCL (poly L-lactide-co-ε-caprolactone) coated bovine bone, sinus elevation

Maxillary sinus augmentation is a predictable technique to increase bone volume in the posterior maxilla prior to implant placement.<sup>1,2</sup> Dental implants placed in sites previously augmented via a lateral wall approach result in an overall implant survival rate of 97.7% after 3 to 6 years.<sup>3</sup>

Different materials were studied, as sole materials or in combination with autogenous bone. Only minor differences in implant survival rate were reported for

autogenous bone combined with various bone substitutes (92% to 94.8%) compared with bone substitutes alone (95.9%).<sup>4</sup> Likewise, Jensen et al<sup>5</sup> reported that implants placed in maxillary sinuses that were augmented with deproteinized bovine bone mineral had a survival rate of 96%, while similar rates (94%) were obtained with a composite graft (20/80 ratio) of autogenous and deproteinized bovine bone mineral graft. However, Froum et al<sup>6</sup> reported significantly greater vital bone formation when as little as 20% of autogenous bone was added to the graft. Also, implants placed in such composite hybrid graft sites had lower annual failure rates compared with bone substitutes alone (1.47% and 2.59%), respectively.

Moreno Vazquez et al<sup>8</sup> reported a low postoperative complication rate (< 15%) in 200 consecutive maxillary sinus augmentation procedures. It should be noted that in the majority of cases, demineralized freeze-dried bovine bone xenograft was used (Bio-Oss, Geistlich). Recently, a novel xenogeneic biomaterial (Bioactive bone, Industrie Biomediche Insubri) was introduced, which is made of bovine bone coated with degradable synthetic poly

<sup>1</sup>Department of Periodontology, School of Graduate Dentistry, Rambam Health Care Campus, Haifa, Israel.

<sup>2</sup>Department of Periodontology, School of Graduate Dentistry, Rambam Health Care Campus, Haifa, Israel; Faculty of Medicine, Technion - Israel Institute of Technology, Haifa, Israel.

**Correspondence to:** Dr Anat Ben-dor, Department of Periodontology, School of Graduate Dentistry, Rambam Health Care Campus, P.O.B 9602, Haifa 31096, Israel. Fax: 972-4-8543057. Email: dr.bendor@gmail.com

Submitted June 30, 2020; accepted February 9, 2021.

©2021 by Quintessence Publishing Co Inc.

List of natural polysaccharides classified according to their origin.

Origin	Polysaccharide
Plants	Starch, cellulose, glucomannan, pectin, hemicellulose, gums, mucilage
Algae	Agar, galactans, alginates, carrageenans
Animals	Chitin, chitosan, hyaluronic acid, glycosaminoglycans, cellulose
Bacteria	Dextran, levan, polygalactosamine, gellan, xanthan, cellulose
Fungal	Elsinan, chitin, chitosan, pollulan, yeast glucans

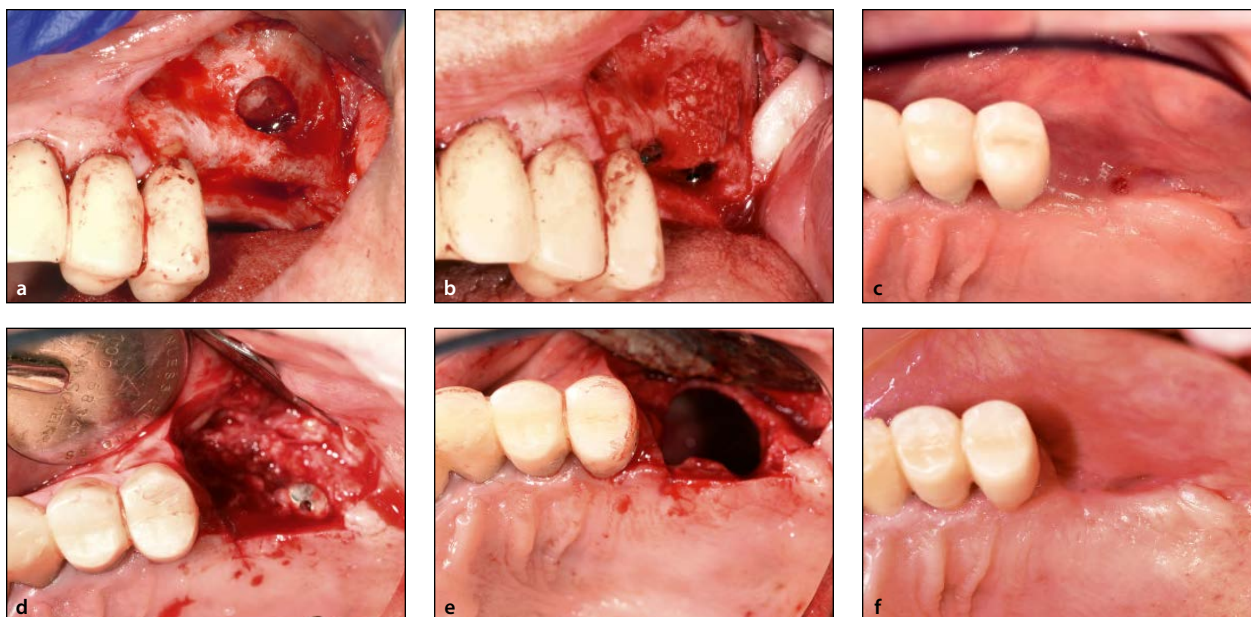


**Fig 1** Clinical appearance of maxillary sinus augmentation complication I. (a) The lateral wall window without perforation of the sinus membrane at the time of maxillary sinus augmentation. (b) One-stage protocol case with placement of implants in the maxillary left first and second molar positions and PLCL bone graft augmentation. (c) 4 months after the procedure, an oroantral sinus tract appeared together with suppuration and exit of bone particles. (d) Reentry surgery revealed extensive inflammation with soft tissue material; the implants were surrounded with soft tissue and complete loss of the buccal bone. (e) Following sinus clearance loss of the buccal bone, there was loss of the implants and huge perforation in the sinus membrane. (f) 3 months after reentry, the complete loss of the buccal bone is evident clinically.

L-lactide-co- $\epsilon$ -caprolactone and natural polysaccharides polymers (PLCL) designed to increase hydrophilicity, cell adhesion, and osteogenicity.<sup>9,10</sup> In a recent in vitro study, this PLCL-coated bovine bone (PBB) was compared with deproteinized bovine bone mineral: Higher vitality and proliferation rate of both mesenchymal stem cells and human osteosarcoma cells were found in the PBB group.<sup>10,11</sup> In another in vivo study of ridge preservation in rats, a higher percentage of new bone and lower residual scaffold were found in the PBB compared with the deproteinized bovine bone mineral control.<sup>11</sup> Histologic analysis of the biopsy specimens demonstrated an intensive new bone formation occurring around this graft, indicating good osteoconduction. Few human cases also reported successful bone reconstruction using PBB.<sup>10</sup>

To the best of the authors' knowledge, this study constitutes the first report of the significant adverse events associated with PBB.

The objective of this retrospective study was to describe the postoperative complications following lateral wall sinus augmentation using PBB. The secondary aims were to examine histologic findings and to propose complication management alternatives.

## MATERIALS AND METHODS

This is a retrospective two-center report of subjects who underwent lateral wall sinus augmentation procedures

using PBB at either the Department of Periodontology, School of Graduate Dentistry, Rambam Health Care Campus, or in one private practice. All cases were treated by highly experienced periodontists (more than 10 years of experience). The study was conducted according to the ethical principles for medical research (IRB approved 0249-19-RMB).

All the patients who underwent unilateral or bilateral open sinus augmentation procedures using PBB alone or simultaneously with implant placement are included in this report (provided that they had a preoperative CBCT taken prior to the procedure and postoperative panoramic radiographs taken immediately postoperatively). Additional panoramic or CBCT images were taken at the time of reported signs or symptoms (5 to 12 months from surgery). Patients with at least a record of two surgical radiographs were included.

A standard lateral wall sinus augmentation protocol was employed (Figs 1a and 1b) with preoperative antibiotics (2 g amoxicillin or 600 mg clindamycin) that was administered 1 hour prior to surgery and followed for an additional 1-week course.

In addition, a single dose of 8 mg dexamethasone was administered 1 hour before the surgery and a daily dose of 4 mg for the first 2 days after surgery along with analgesics as necessary. The patients received postoperative instructions that included mouthrinse with chlorhexidine gluconate 0.2% for 3 weeks.

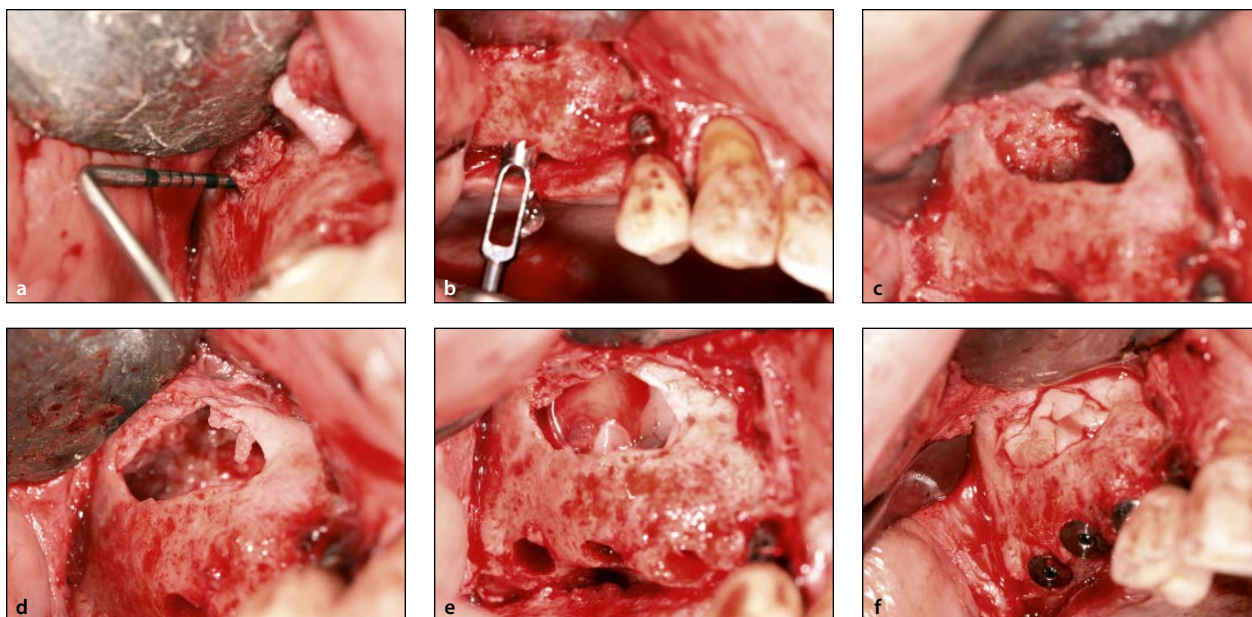


**Fig 2** Clinical appearance of maxillary sinus augmentation complication II. (a) 8 months following the procedure, probing in the lateral wall demonstrated soft tissue material in the sinus cavity. (b) Trepine biopsy specimen was taken from maxillary right first molar that included the residual bone ridge and the augmentation material from the sinus cavity. (c, d) Following sinus clearance, a dense solid tissue was evident instead of the sinus membrane, with no perforation separating the surgical compartment from the maxillary sinus above. (e) Three osteotomes were performed in maxillary right second premolar and first and second molar positions and the sinus cavity was filled with LPRF membranes. (f) Three implants were placed with good primary stability.

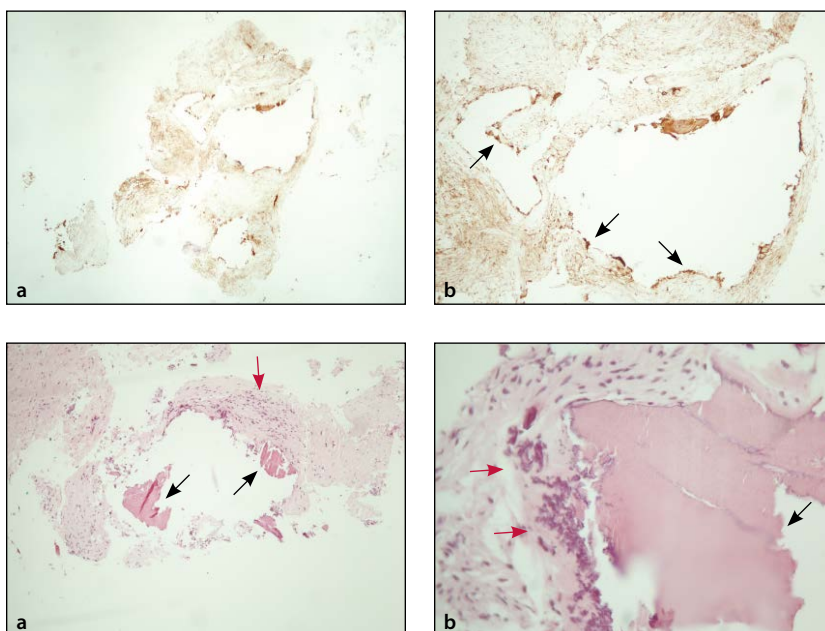


**Fig 3** CD68 immunostaining of tissue biopsy specimens retrieved from the maxillary sinus cavity following augmentation. (a) Magnification 40x; (b) Magnification 100x; black arrows point at cells originating from the macrophage lineage (histocyte cells).

**Fig 4** Hematoxylin and eosin staining of tissue biopsy specimens retrieved from the maxillary sinus cavity following augmentation. (a) Magnification 40x; (b) magnification 200x; black arrows point at residual xenograft particles; red arrows point at inflammatory reaction.

Suture removal was performed 2 weeks postoperatively, and follow-up visits were performed at 6 weeks, 3 months, and 6 months following the surgical procedure. Implant placement in these sites was performed either with sinus augmentation or 6 to 9 months postoperatively.

In cases that presented complications (see the results section), additional antibiotic therapy was prescribed, and if this failed to resolve the problem, the implants were explanted. In persistent cases, a reentry

surgery was performed, in which the lateral window was exposed, and the infected grafting material was completely removed. In two of those persistent cases, biopsy specimens were taken from the sinuses during the reentry surgery. In one asymptomatic case 8 months after sinus augmentation, a core biopsy specimen was obtained by using a trephine bur during osteotomy preparation for implant placement (Fig 2b). The histologic slides were stained with hematoxylin and

**Table 1** Characteristics of Symptoms in Complication Cases

Characteristics	N	%
Pain	15	68.2
Implant failure	15	68.2
Swelling	14	63.6
Oroantral fistula	12	54.5
Sensitivity to palpation	8	36.4
Suppuration	8	36.4
Lateral sinus wall resorption	7	31.8
Radiographic radiolucency/pathology	7	31.8
Implant mobility	6	27.3
Redness	4	18.2
Halitosis	4	18.2
Runny nose	4	18.2
Bad taste	3	13.6
Exit of bone particles	3	13.6
Radiographic graft resorption	3	13.6
Wound dehiscence	2	9.1
Deep probing pocket depth around the implant	2	9.1
Patients with complications	18	29.5

eosin solution (Fig 3a) and with immunohistochemistry to identify CD68 (Fig 4a), a marker for cells of the macrophage lineage. Furthermore, a microbial sampling was taken during one of the reentry surgeries.

## RESULTS

A total of 67 sinuses in 61 patients were included in the study. Patients' ages ranged from 29 to 83 years, with a mean age of  $60.1 \pm 11.16$  years. Fifty-four percent of patients were women (28 men and 33 women). Three patients (4.92%) were light smokers (< 10 cigarettes a day).

Fifty-five patients received unilateral and six patients received bilateral lateral wall sinus augmentation procedures. The prevalence of postoperative complications was 29.5% in patient-based calculation (18 patients out of 61) and 32.8% in sinus-based calculation (22 sinuses out of 67). Of those complications, 59.1% occurred in two-stage cases and 40.9% occurred in one-stage cases.

Symptom appearance ranged from 2 to 19 months (mean:  $8.38 \pm 4.9$  months). The most prevalent symptoms were persistent pain, swelling, and oroantral fistula (Table 1; Fig 1c); those occurred in > 50% of the patients. Radiographic signs appeared in 45.5% of the complications and included partial or complete disappearance of the graft (13.6%) and radiolucency within the grafting material (31.8%; Figs 5b and 5d) or surrounding the implants (Figs 6d and 6e). In most cases, failures presented themselves by implant spontaneous exposure, mobility, oroantral fistula, or deep probing pocket depth following implant restoration.

For the sinuses that presented with complications (22 sinuses), 24 implants in 15 sinuses have failed, resulting in a 20.1% survival rate in those sinuses.

All 22 failing sinuses were operated on by three surgeons. An interoperator comparison showed that the failure rate was comparable: E.E.M., 27.3% (6/22 sinuses), E.G., 33.3% (5/15 sinuses), and Y.M., 36.7% (11/30 sinuses).

## Management of Complications

The initial treatment in 63.6% of the cases was a prescription of a second antibiotic course; this resulted in a temporary improvement. One case was treated with chlorhexidine lavage via the oroantral fistulation. In 36.4% of the cases, implants were removed (Figs 1d and 1e). The aforementioned treatments did not solve the problems in most of the cases, and therefore, a reentry procedure was needed in 19 cases (86.4%). Following flap elevation and lateral window exposure, the sinus was exposed. It was found to be full with granulation tissue surrounding pieces of a nonossified rubber-like material (Figs 2a and 7a). Some cases presented widespread inflammation, inflamed sinus membrane, and severe resorption of the buccal plate and the bone crest (Figs 1e and 6f). In cases where implants were placed, nonosseointegrated implants were surrounded by soft tissue (Fig 1d). In most cases, the sinus was cleaned thoroughly; the graft material remnants were removed together with inflamed parts of the sinus membrane, followed by chlorhexidine and saline lavages (Fig 7b).



**Fig 5** Radiographic appearance of maxillary sinus augmentation complication III. (a) CBCT before maxillary sinus augmentation. (b) CBCT 9 months following the procedure. (c) CBCT immediately following the reentry surgery that included sinus clearance from granulation tissue. A dome shape was evident in the superior aspect of the augmentation with a communication area to the sinus cavity. A collagen membrane was applied on that area. LPRF membranes were used to fill the sinus cavity, and another collagen membrane was applied on the lateral window. No bone was augmented at this stage. Note the significant thickening of the sinus membrane. (d) CBCT 6 months following sinus clearance. Partial bone fill was evident; however, the communication area to the sinus was still evident. (e) Panorex immediately following second maxillary sinus augmentation procedure. The procedure was performed guided, and implants were placed in the maxillary left first and second molar positions in the areas filled with bone.

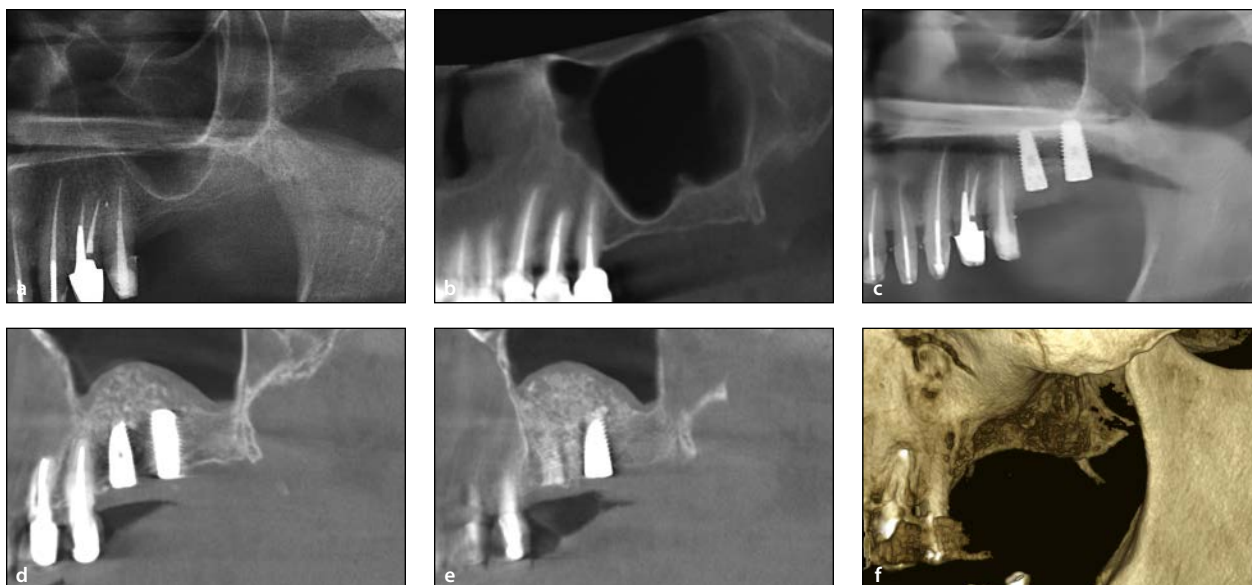


**Fig 6** Radiographic appearance of maxillary sinus augmentation complication I. (a) Panorex before maxillary sinus augmentation. (b) CBCT before the procedure. (c) Panorex following the procedure. (d, e) CBCT 6 months following the procedure demonstrating radiolucency surrounding the implants in maxillary left first and second molar positions. (f) Radiographic appearance in 3D bone model CBCT following 6 months from reentry surgery demonstrating complete loss of the buccal bone.

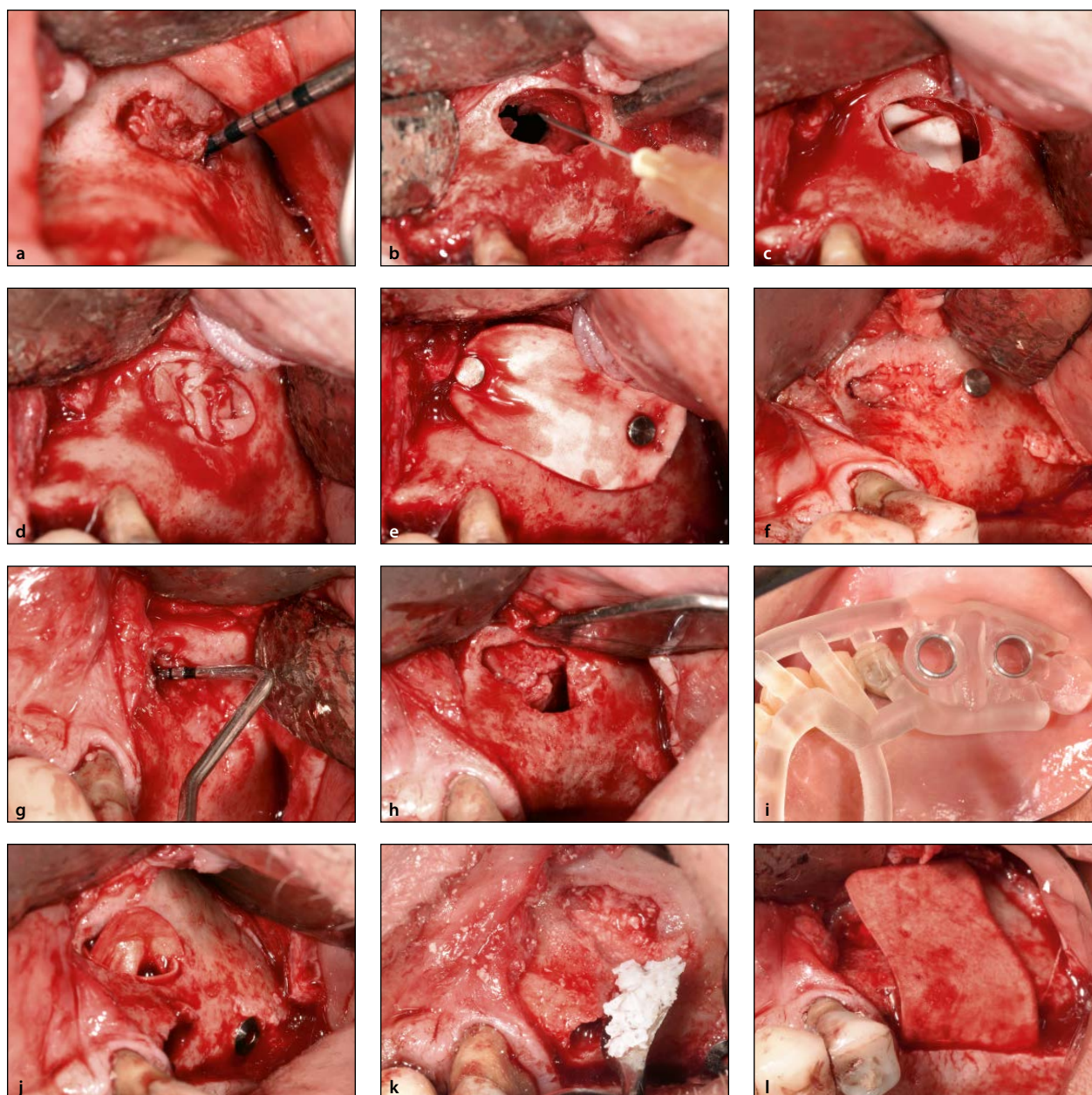


**Fig 7** Clinical appearance of maxillary sinus augmentation complication III. (a) 9 months following the procedure, probing in the lateral wall demonstrated soft tissue material in the sinus cavity. (b) Following sinus clearance, a dense solid tissue was evident instead of the sinus membrane with big communication to the sinus cavity. The sinus was washed with saline. (c) A collagen membrane was applied on the communication. (d) LPRF membranes filled the compartment. (e) Another collagen membrane was applied on the lateral window. Primary closure was achieved. (f) 7 months later, reentry surgery was performed. (g) The sinus cavity was not completely filled bone as expected, and the communication area to the sinus was still evident. (h) The sinus membrane was very thick but not hard as before. (i) The procedure was performed guided, and implants were placed in the maxillary left first and second molar positions in the areas filled with bone. (j) Again, a collagen membrane was applied on the communication area. (k) Repeated sinus augmentation using xenograft (Bio-Oss). (l) Another collagen membrane was applied following implant placement in the maxillary left first and second molar positions.

### Histology

Two biopsy specimens were taken from asymptomatic patients who presented radiographic radiolucency in the grafted sinus. Histologic analysis revealed mainly mild chronic inflammation (Figs 3a and 3b), fragments of xenograft, loose connective tissue, and fibro-adipose tissue. No vital bone was evident (Figs 4a and 4b).

One biopsy specimen was taken from a patient with an acute sinus infection. In this case, severe inflamed fibrous tissue surrounded the residual graft lacking vital bone, and focal cholesterol clefts, giant cells, and granulation tissue were found in the histologic slide. In microbial sampling, no anaerobic bacteria could be detected in the culture; also, no bacteria growth was

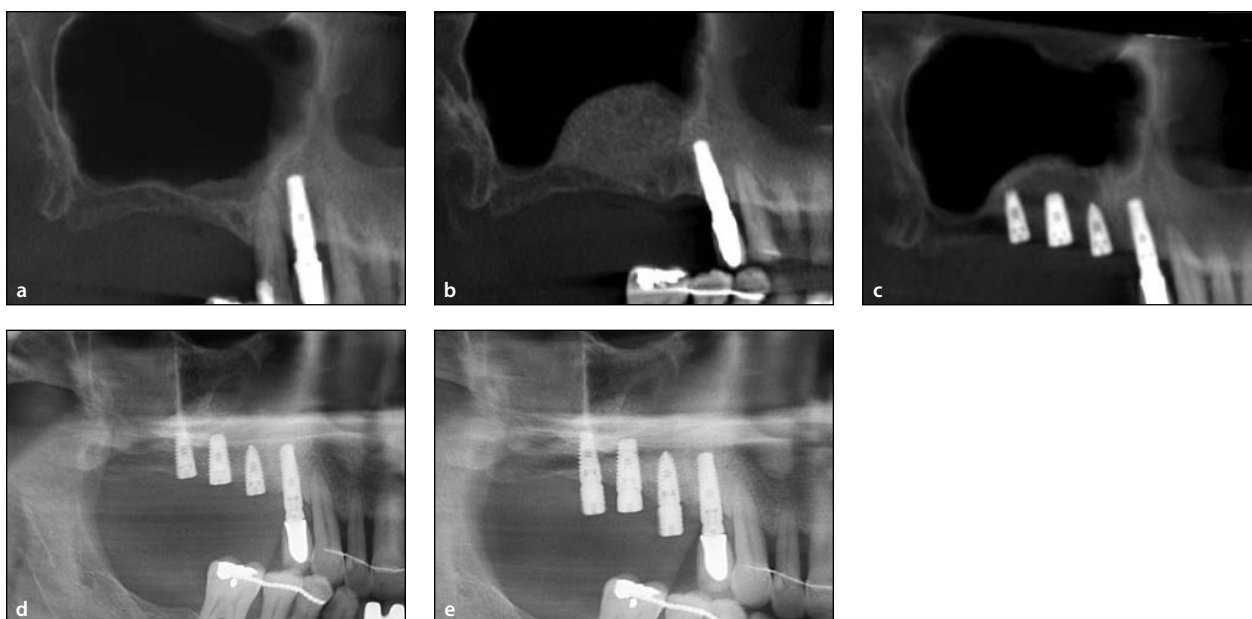


**Fig 8** Radiographic appearance of maxillary sinus augmentation complication II. (a) CBCT before maxillary sinus augmentation. (b) CBCT 9 months following the procedure. (c) CBCT 1 month following reentry surgery. The surgery included implant placement in the maxillary right second premolar and first and second molar positions with LPRF membranes to fill the sinus cavity. The dome shape is evident in the superior aspect of the augmentation. (d) Panorex immediately following the reentry surgery. (e) Panorex following stage-two surgery, 6 months following reentry surgery, demonstrating good primary stability of all the implants with no pathologies.

found in the direct smear. However, *Streptococcus salivarius* was found. 

## DISCUSSION

In the present retrospective analysis, an overall 32.8% postoperative complication rate was documented following lateral wall sinus augmentation using PBB.

Infection of the grafted sinus is generally considered a rare complication, with a mean incidence of 2.9% (range: 0% to 7.4%).<sup>7</sup> This usually develops 3 to 7 days postsurgically. However, > 20% of the present cases using PBB presented signs of active infection (such as orofacial fistula and suppuration), which correspond to at least 7-times-higher incidence of infections compared with the literature.<sup>7,12</sup>

Askar et al<sup>13</sup> use the six-level postoperative classification system to assess the incidence and severity of postoperative complications following dental surgical procedures. It was found that patients who underwent lateral wall sinus augmentation had a 30% chance to develop some type of complication. Similarly, in the present study, the patients had a complication rate of 29.5%.

Regarding the severity of complications, it seems that in the present study, the Grade III complication rate is 1.7-fold higher (24.6% in comparison to 14.3%).

The implant survival rate was reported to be 90% to 97.7% following 3 to 6 years of function.<sup>3,7,12</sup> However, in the present study, the implant survival rate was 80.3% following 19 months, which is significantly lower.

Infection is considered the leading cause of implant failure since 61.4% of failed implants were reported to have an infection.<sup>14</sup> In the present study, 79.9% of the implants in infected sinuses failed, a much higher rate than reported in the literature following infections.<sup>14</sup>

Other postoperative complications were also higher than in previous publications.<sup>15,16</sup>

In three cases, implants have not yet been placed, so further complications might still occur. The complications were detected within a variable time range and could be detected even following more than a year and a half. Therefore, the authors expect to have more complications in the future.

The failures presented a spectrum of symptoms and could be detected radiographically in < 50% of the cases. Pain and implant failure were the most prevalent complications (68.2% and 68.2%, respectively).

Few cases presented a dome-shape appearance, known as the “Dome Phenomenon” (Figs 2c and 2d), which was detected during the reentry procedure and was also evident radiographically (Fig 8c).<sup>17</sup> Mahler et al reported that after removal of infected grafting material and resolution of the inflammation, the bony dome may present itself in the apical extension of the

previously grafted area. The present study, therefore, left the “dome-shape” solid tissue in the sinuses following reentry and filled the sinus with LPRF membranes (Figs 2e and 2f). However, in the present cases, this did not ossify (Figs 7g and 7h). One case required a second reentry surgery, and therefore, the authors might recommend in those cases a complete removal of the sinus content during reentry (Figs 5c and 5d).

Biopsy specimens demonstrated histologically severe inflamed fibrous tissue with giant cells or mild chronic inflammation with loose fibrin-connective tissue and fibro-adipose tissue.

There were no histologic features of new bone formation around the grafted material.

Several limitations should be noted in this study. First, it was a retrospective study. There are different specialists who performed the procedure, and therefore, the technique was not uniform.

Reports of multiple failures following sinus augmentations are rare. One study<sup>18</sup> reported multiple implant failures following the use of demineralized bone matrix allograft in maxillary sinus augmentation. Biopsy specimens taken from the failed sinuses during reentry demonstrated mild to severe inflammatory reactions, and histologic examination revealed no features of new bone formation around the graft. The results reported there are very similar to the present study, especially the histopathologic picture.

## CONCLUSIONS

Lateral wall maxillary sinus augmentation using PBB was associated with a histologic appearance of acute sinus infection and with a 7-times-higher failure rate compared with previous reports and only an 80.2% implant survival rate. This serious adverse event suggests that PBB cannot be recommended for maxillary sinus augmentations.

## ACKNOWLEDGMENTS

The authors report no conflicts of interest related to this study, which was self-supported by the authors.

## REFERENCES

- Boyne PJ, James RA. Grafting of the maxillary sinus floor with autogenous marrow and bone. *J Oral Surg* 1980;38:613–616.
- Tatum H Jr. Maxillary and sinus implant reconstructions. *Dent Clin North Am* 1986;30:207–229.
- Antonoglou GN, Stavropoulos A, Samara MD, et al. Clinical performance of dental implants following sinus floor augmentation: A systematic review and meta-analysis of clinical trials with at least 3 years of follow-up. *Int J Oral Maxillofac Implants* 2018;33:e45–e65.
- Aghaloo TL, Moy PK. Which hard tissue augmentation techniques are the most successful in furnishing bony support for implant placement? *Int J Oral Maxillofac Implants* 2007;22(suppl):49–70.
- Jensen T, Schou S, Stavropoulos A, Terheyden H, Holmstrup P. Maxillary sinus floor augmentation with Bio-Oss or Bio-Oss mixed with autogenous bone as graft: A systematic review. *Clin Oral Implants Res* 2012;23:263–273.
- Froum SJ, Tarnow DP, Wallace SS, Rohrer MD, Cho SC. Sinus floor elevation using anorganic bovine bone matrix (OsteoGraf/N) with and without autogenous bone: A clinical, histologic, radiographic, and histomorphometric analysis—Part 2 of an ongoing prospective study. *Int J Periodontics Restorative Dent* 1998;18:528–543.
- Pjetursson BE, Tan WC, Zwahlen M, Lang NP. A systematic review of the success of sinus floor elevation and survival of implants inserted in combination with sinus floor elevation. *J Clin Periodontol* 2008;35(suppl 8):216–240.
- Moreno Vazquez JC, Gonzalez de Rivera AS, Gil HS, Mifsut RS. Complication rate in 200 consecutive sinus lift procedures: Guidelines for prevention and treatment. *J Oral Maxillofac Surg* 2014;72:892–901.
- Pertici G, Rossi F, Casalini T, Perale G. Composite polymer-coated mineral grafts for bone regeneration: Material characterisation and model study. *Ann Maxillofac Surg* 2014;14:4.
- Pertici G, Carinci F, Carusi G, et al. Composite polymer-coated mineral scaffolds for bone regeneration: From material characterization to human studies. *J Biol Regul Homeost Agents* 2015;29(suppl 1):136–148.
- Mayer Y, Ginesin O, Khutaba A, Machtei EE, Zigdon Giladi H. Biocompatibility and osteoconductivity of PLCL coated and noncoated xenografts: An in vitro and preclinical trial. *Clin Implant Dent Relat Res* 2018;20:294–299.
- Wallace SS, Froum SJ. Effect of maxillary sinus augmentation on the survival of endosseous dental implants. A systematic review. *Ann Periodontol* 2003;8:328–343.
- Askar H, Di Gianfilippo R, Ravida A, Tattan M, Majzoub J, Wang HL. Incidence and severity of postoperative complications following oral, periodontal, and implant surgeries: A retrospective study. *J Periodontol* 2019;90:1270–1278.
- Katranji A, Fotek P, Wang HL. Sinus augmentation complications: Etiology and treatment. *Implant Dent* 2008;17:339–349.
- Fugazzotto P, Melnick PR, Al-Sabbagh M. Complications when augmenting the posterior maxilla. *Dent Clin North Am* 2015;59:97–130.
- Zijderveld SA, van den Bergh JP, Schulten EA, ten Bruggenkate CM. Anatomical and surgical findings and complications in 100 consecutive maxillary sinus floor elevations. *J Oral Maxillofac Surg* 2008;66:1426–1438.
- Mahler D, Levin L, Zigdon H, Machtei EE. The “dome phenomenon” associated with maxillary sinus augmentation. *Clin Implant Dent Relat Res* 2009;11(suppl 1):e46–e51.
- Lee SS, Jang JH, Kim KS, Yoo YJ, Kim YS, Lee SK. Failure of bone regeneration after demineralized bone matrix allograft in human maxillary sinus floor elevation. *Basic Appl Pathol* 2009;2:125–130.

See discussions, stats, and author profiles for this publication at: <https://www.researchgate.net/publication/229925344>

# Fast Degradable Poly(L-lactide-co-??-caprolactone) Microspheres for Tissue Engineering: Synthesis, Characterization, and Degradation Behavior

Article in *Journal of Polymer Science Part A Polymer Chemistry* · July 2007

DOI: 10.1002/pola.22031

CITATIONS

76

READS

1,446

4 authors:



**Kalpna Garkhal**

Vyome Biosciences

8 PUBLICATIONS 255 CITATIONS

[SEE PROFILE](#)



**Shalini Gohil**

10x Genomics

27 PUBLICATIONS 679 CITATIONS

[SEE PROFILE](#)



**Kamal Jonnalagadda**

University of the Sciences in Philadelphia

34 PUBLICATIONS 635 CITATIONS

[SEE PROFILE](#)



**Neeraj Kumar**

National Institute of Pharmaceutical Education and Research

90 PUBLICATIONS 3,467 CITATIONS

[SEE PROFILE](#)

Some of the authors of this publication are also working on these related projects:



Tideglusib Formulation [View project](#)



Polymer drug system [View project](#)

# Fast Degradable Poly(L-lactide-co- $\epsilon$ -caprolactone) Microspheres for Tissue Engineering: Synthesis, Characterization, and Degradation Behavior

KALPNA GARKHAL,<sup>1</sup> SHALINI VERMA,<sup>1</sup> S. JONNALAGADDA,<sup>2</sup> NEERAJ KUMAR<sup>1</sup>

<sup>1</sup>Department of Pharmaceutics, National Institute of Pharmaceutical Education and Research, Sec. 67, SAS Nagar, Mohali 160062, India

<sup>2</sup>Department of Pharmaceutical Sciences, Philadelphia College of Pharmacy, University of the Sciences in Philadelphia, 6005 43rd Street, Philadelphia, Pennsylvania 19104

Received 16 June 2006; accepted 10 February 2007

DOI: 10.1002/pola.22031

Published online in Wiley InterScience (www.interscience.wiley.com).

**ABSTRACT:** Polymeric scaffolds play a crucial role in engineering process of new tissues and effect the cell growth and viability. PLCL copolymers are found to be very useful during cell growth due to their elastic behavior and mechanical strength. Thus, low molecular weight PLCL copolymers of various ratios viz. PLCL(90/10), PLCL(75/25), PLCL(50/50) and PCL were synthesized by ring opening polymerization using stannous octoate as a catalyst. Synthesized polymers were characterized by GPC, <sup>1</sup>H-NMR, FTIR and XRD. The thermal properties of the copolymers were studied using TGA and DSC. Microspheres of about 100  $\mu$ m diameter were prepared for different copolymers and their *in vitro* degradation behaviors were studied up to 108 days. It was observed that degradation of PLA content in polymer backbone occurs faster than PCL component which is also indicated by corresponding change in ratios of PLA/PCL, as determined by <sup>1</sup>H-NMR. SEM images of microspheres depicted the surface morphology during degradation and suggested the faster degradation for PLCL (50:50). Copolymers of different thermal, mechanical properties and different degradation behaviors can be prepared by adjusting the composition of copolymers. Various synthesized polymers from this work have been tested in our laboratory as polymeric scaffold for soft tissue engineering. © 2007 Wiley Periodicals, Inc. *J Polym Sci Part A: Polym Chem* 45: 2755–2764, 2007

**Keywords:** biodegradable; biopolymers; copolymerization; degradation; degradation behavior; microspheres; polyesters; poly(lactide-co- $\epsilon$ -caprolactone); ring opening polymerization

## INTRODUCTION

During the last few decades, clinical needs have motivated biomedical applications of biodegradable polymers in the field of tissue engineering, surgery, and drug delivery. Currently used biodegradable

polymers include polyesters, polyanhydrides, polyhydroxyalkanoates, polyphosphazenes, and their copolymers.<sup>1–5</sup> Polymers used in tissue engineering serve as a physical support for seeded cells and provide a template for three-dimensional organization to enable cell adhesion, migration, proliferation, differentiation, and eventually tissue regeneration.<sup>3,4</sup> The coordination of polymer degradation rate with cellular biosynthetic rates and cell seeding characteris-

Correspondence to: N. Kumar (E-mail: neeraj@nipr.ac.in)

*Journal of Polymer Science: Part A: Polymer Chemistry*, Vol. 45, 2755–2764 (2007)  
© 2007 Wiley Periodicals, Inc.

tics of polymer is critical for the success of an engineered tissue construct. Therefore degradation behavior of scaffolds plays a crucial role in the engineering process of new tissue and affects cell growth and viability.<sup>3</sup>

Polycaprolactone (PCL), one among the few polyesters that have been extensively explored for tissue engineering applications, has been researched for use as a carrier for drug delivery systems for long term release kinetics<sup>6,7</sup> and in the form of absorbable sutures. PCL is relatively nontoxic, and possesses sufficient mechanical strength, biocompatibility, and thermal stability for scaffolding applications. A low glass transition temperature of about  $-60\text{ }^{\circ}\text{C}$  provides a rubbery consistency at room temperature, offering potential for load-bearing applications in tissue engineering.<sup>4</sup> PCL has been used in the engineering of cartilage, bone, skin,<sup>4,8,9</sup> smooth muscle cells,<sup>4,10,11</sup> heart valve, axonal regeneration,<sup>4</sup> and so forth. Scaffolding devices previously explored for tissue engineering applications include films,<sup>12</sup> sponges, meshes, fibers<sup>13,14</sup>, hydrogels,<sup>15–17</sup> and microspheres.<sup>18</sup> A major limitation in the use of PCL is its slow degradation rate owing to high hydrophobicity and crystallinity. Consequently, PCL has been used as a physical blend with polysaccharides, cellulose propionate, cellulose acetate butyrate, poly(lactic acid), poly(lactic-co-glycolic acid) and PEG.<sup>4,6,19,20</sup> Copolymers of PCL have also been investigated with L-lactide, DL-lactide, and glycolide for use in drug delivery and tissue engineering.<sup>7,21,22</sup> While L-lactide and  $\epsilon$ -caprolactone (PLCL) copolymers have been reported previously,<sup>2,21</sup> their use in soft tissue engineering is limited by a long degradation time in the range of 2–3 years, possibly due to a high molecular weight (generally  $>100\text{ kDa}$ <sup>23</sup>).

In this study, we report the synthesis and characterization of low molecular weight random PLCL copolymers of varying copolymeric ratios followed by *in vitro* degradation studies of microsphere scaffolds fabricated thereof. These microsphere scaffolds were further modified using a biomimetic peptide (P-15) and tested *in vitro*, the results of which have been reported elsewhere.<sup>24</sup> The lower molecular weight was expected to result in lower degradation times and crystallinity, thereby improving suitability for soft tissue engineering applications. *In vitro* degradation behavior of PLCL microsphere scaffolds was evaluated in phosphate buffer (pH 7.4) at  $37\text{ }^{\circ}\text{C}$ , and compared with that of PCL homopolymer. Changes in mass, molecular weight, polymer

composition, polymer crystallinity, and surface morphology following degradation are reported.

## MATERIALS AND METHODS

### Materials

$\epsilon$ -Caprolactone was purchased from Fluka and distilled over calcium hydride. Stannous octoate was obtained from Sigma and purified by distillation. L-lactide was purchased from Purac and used as received.

### Synthesis of Poly(L-lactide-co- $\epsilon$ -caprolactone)

PLCL was synthesized by ring opening polymerization (ROP) at  $140\text{ }^{\circ}\text{C}$  for 16 h. L-Lactide, distilled  $\epsilon$ -caprolactone, and 0.2% w/w stannous octoate were introduced into a round-bottomed flask, followed by nitrogen purging to provide an inert environment during polymerization. After polymerization, the reaction was stopped by cooling the product in ice. The resulting polymer was dissolved in dichloromethane (DCM) and precipitated four times using excess isopropyl alcohol. The precipitated PLCL was filtered and dried in a vacuum oven at  $50\text{ }^{\circ}\text{C}$ . The polymerization reaction was carried out using different monomeric ratios to obtain PLCL copolymers of varying lactide/caprolactone ratios of 50/50, 75/25, 90/10, and 0/100 respectively.

### Characterization

The molecular weight of the random poly(L-lactide-co- $\epsilon$ -caprolactone) copolymer was characterized using gel permeation chromatography (GPC). The equipment comprised a Shimadzu LC-10AT VP HPLC pump and Shimadzu SIL-10AD VP refractive index detector. A Shimadzu and Styragel<sup>®</sup> HR3 and HR4 column ( $7.8 \times 300\text{ mm}$ ) was used. Calibration was performed using polystyrene standards (Polysciences) in chloroform at  $30\text{ }^{\circ}\text{C}$ , and elution rate  $1\text{ mL/min}$ . <sup>1</sup>H-NMR spectra were recorded with Avane DPX 300, Bruker, using  $\text{CDCl}_3$  as solvent. FTIR spectra were recorded in a Perkin-Elmer IR spectrometer on solvent cast polymer films on NaCl plate. Chloroform was used as the solvent for film casting. Thermal analysis was performed using a Perkin-Elmer, Diamond DSC and differential scanning calorimeter with intercooler 1P cooling accessory. Copolymer samples up to 5 mg

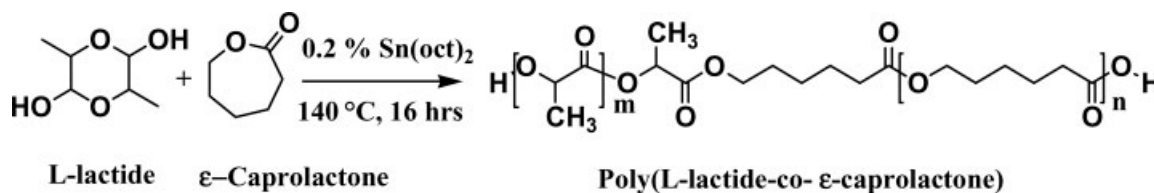


**Figure 1.** Synthesis of poly(L-lactide-co-ε-caprolactone) copolymer.

were heated under nitrogen atmosphere at a heating rate of 10 °C/min. Thermal gravimetric analysis (TGA) was performed using Mettler Toledo, TGA/SDTA 851<sup>e</sup>.

### Microspheres Preparation

Polymer microspheres were prepared using a solvent evaporation technique described previously.<sup>25</sup> Briefly, 200 mg PLCL was dissolved in 4 mL of DCM (nonaqueous phase), and added dropwise into 80 mL of 1% polyvinyl alcohol (PVA) solution (aqueous phase) with high agitation at 600 rpm to enable formation of an o/w emulsion. Stirring was continued overnight to evaporate DCM. Microspheres were recovered by centrifugation at 3000g, washed three times with distilled water, and dried in vacuum oven at 60 °C. The ratio of organic to aqueous phase and stirring rate were maintained constant, while the polymer and PVA concentration were varied so as to achieve a desired microsphere diameter of about 100 μm.

### In Vitro Degradation Studies

Microspheres (20 mg) were suspended in 1 mL of phosphate buffer (0.1 M, pH 7.4) with 0.02% (w/v) sodium azide (NaN<sub>3</sub>) as bacteriostatic and placed in a shaking water bath at 37 °C and 100 rpm ( $n = 4$ ). After predetermined intervals, namely, 0 h, 4 days, and on weekly intervals up to 16 weeks, samples were centrifuged at

2350 g for 5 min to separate microspheres from supernatant degradation medium. The supernatant was analyzed for changes in pH. The palletized microspheres were vacuum-dried to constant weight, and final weight determined to measure weight loss. The dried microspheres were further analyzed by GPC, FTIR, <sup>1</sup>H-NMR, XRD, and DSC to observe the effect of degradation on molecular weight, composition and other polymer properties.

## RESULTS AND DISCUSSION

### Synthesis of Poly(L-lactide-co-ε-caprolactone)

Random copolymer of PLCL was synthesized by ROP using stannous octoate as catalyst (Fig. 1) with a yield of 85%–90% for various ratios of copolymers (Table 1). At temperatures below 140 °C, the incorporation of CL units into polymer chains was incomplete because of the low reactivity of CL.<sup>26</sup> The polymerization conditions for different copolymer ratios were kept same as mentioned above while different ratio of monomers were used to get the polymers with different physical properties as shown in Table 1. Copolymer PLCL (50/50) exhibited the consistency of a gummy solid, while PLCLs with higher lactide ratios showed a stronger consistency. These results suggest that the stiff PLLA may be toughened by incorporating PCL as a flexible, elastic polymer so as to make the copolymer more con-

**Table 1.** Characteristics of Polymers

Polymer (LA/CL ratio)	LA/CL <sup>a</sup>	$M_n^b$ (kDa)	$M_w^b$ (kDa)	$\Delta H^c$ (J/g)	$T_m^c$ (°C)	$T_d^d$ (°C)	Yield (%)
PCL (0/100)	0/100	46.79	72.44	90.3	65.1	396	77.9
PLCL (50/50)	48/52	22.38	33.41	–	–	360	80.8
PLCL (75/25)	74.1/24.9	30.61	53.11	22.3	145.8	320	88.6
PLCL (90/10)	91.7/8.3	59.94	97.32	39.1	167.4	316	89.5

<sup>a</sup>Molar ratio of L-lactide/ε-caprolactone determined from <sup>1</sup>H NMR.

<sup>b</sup>Molecular weight determined by GPC.

<sup>c</sup>Data obtained by DSC.

<sup>d</sup>Decomposition temperature determined by TGA.

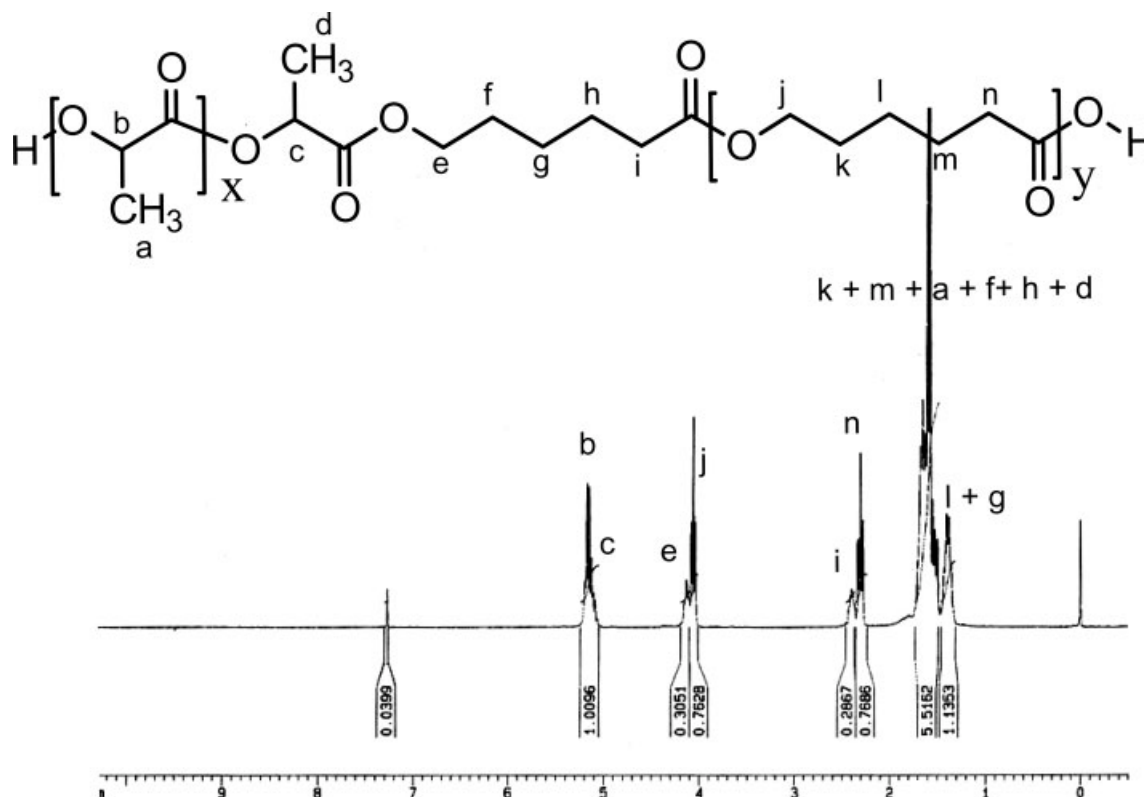


Figure 2.  $^1\text{H-NMR}$  spectra for PLCL (50/50) copolymer.

ductive to scaffold fabrication and related biomedical applications.<sup>10,26,27</sup>

Molecular weights of copolymers as characterized by GPC are reported in Table 1. The polydispersity index was in the range of 1.5–1.6. Both the number and weight average molecular weights of synthesized PLCL copolymers increased with increasing LA content, probably due to the higher reactivity of LA units during copolymerization.<sup>21</sup>

The  $^1\text{H-NMR}$  spectrum of PLCL (50/50) showed signals at  $\delta 1.57$  ( $\text{CH}_3$ , PLLA),  $\delta 5.1$  ( $\text{CH}$ , PLLA),  $\delta 1.35$ – $1.67$  ( $\text{CH}_2\text{CH}_2\text{CH}_2$ , PCL),  $\delta 2.3$  ( $\text{CH}_2\text{CO}$ , PCL) and  $\delta 4.03$  ( $\text{CH}_2\text{O}$ , PCL). Other ratios of PLCL copolymer showed similar patterns in  $^1\text{H-NMR}$  spectra except for variation in their integration values for various peaks. Signals characteristic to LA-CL junctions in PLCL copolymer were detected at 2.4, 4.1, and 5.0 ppm in the NMR spectra of various ratios which indicates the involvement of transesterification reactions<sup>2</sup> for the formation of random copolymer (Fig. 2). The LA/CL molar ratio in the PLCL copolymers was calculated using the integration ratio of peaks at 5.1 ppm for LA unit and at 4.0 ppm for CL unit.

FTIR spectra of PLCL(50/50) exhibits carbonyl stretching ( $\text{C}=\text{O}$ ) at  $1757\text{ cm}^{-1}$  (due to PLA block),  $1736.7\text{ cm}^{-1}$  (due to PCL block) while other copolymers studied gave a single peak at  $1757\text{ cm}^{-1}$  as shown in Figure 3. When width of carbonyl stretch was compared among PCL and other copolymers, widening of band was observed with an increase in CL component in various ratios. This may be due to merging of two peaks into one as a result of randomness of copolymers.<sup>27,28</sup> On the other hand, PLCL(50/50) gave one splitting peak due to equal components for both the monomers. C—O band in region of  $1000$ – $1300\text{ cm}^{-1}$  demonstrates the presence of ester group and strong band at  $1184\text{ cm}^{-1}$  shows ester of long alkyl chain in polymer structure. Bands at  $2990$  (PLA),  $2945$  and  $2860\text{ cm}^{-1}$  (PLA and PCL) were present due to alkyl groups in copolymers of PLCL.<sup>2,27</sup> Absence of band at  $2990\text{ cm}^{-1}$  in PCL is in agreement with the statement that CH stretching at  $2990\text{ cm}^{-1}$  was characteristic of PLA component present in all ratios of PLCL copolymers.

DSC exhibited a broad melting transition in the range of  $65.1$ – $167.4\text{ }^\circ\text{C}$  and showed an increasing trend in melting point with an increase

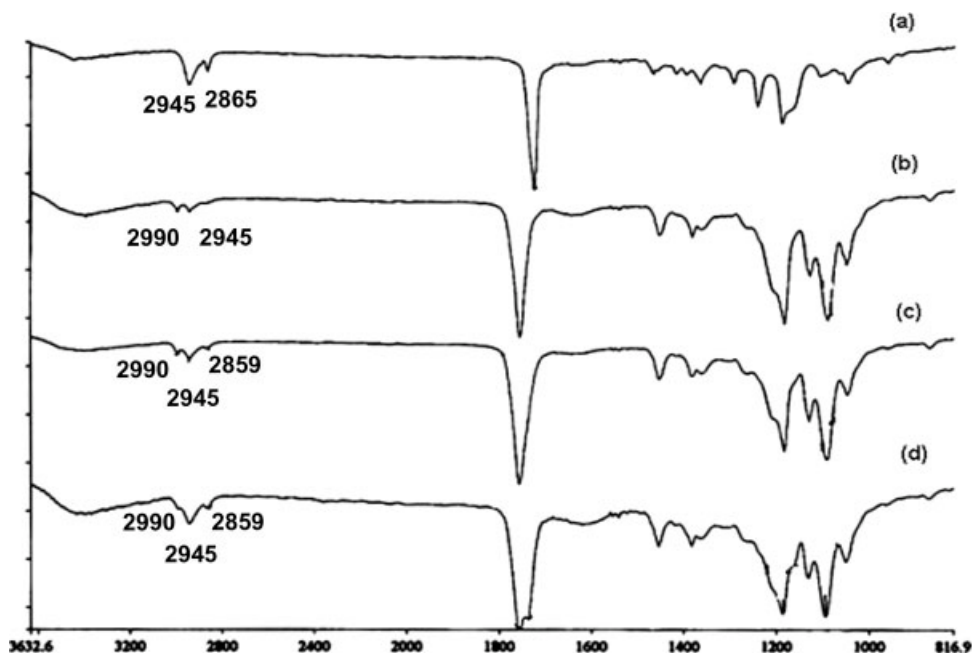


**Figure 3.** FTIR spectra of (a) PCL, (b) PLCL(90/10), (c) PLCL(75/25), and (d) PLCL(50/50).

in LA content in the copolymer. Melting point of PLCL (75/25) and PLCL (90/10) were 145.8 and 167.4 °C respectively, which were between the melting points of PLA (m.p. 180 °C)<sup>29</sup> and PCL (m.p. 65 °C), due to randomization of two blocks together. PLCL(90/10) XRD spectra exhibited

two main diffraction peaks at  $2\theta$  angles of 16.8 and 19.1 along with other peaks which are characteristics of  $\alpha$  crystal cell of PLLA (Fig. 4). XRD spectra of copolymers did not show the characteristic peaks of PCL at 21.6 and 23.6. All the copolymers except PLCL(50/50) showed an

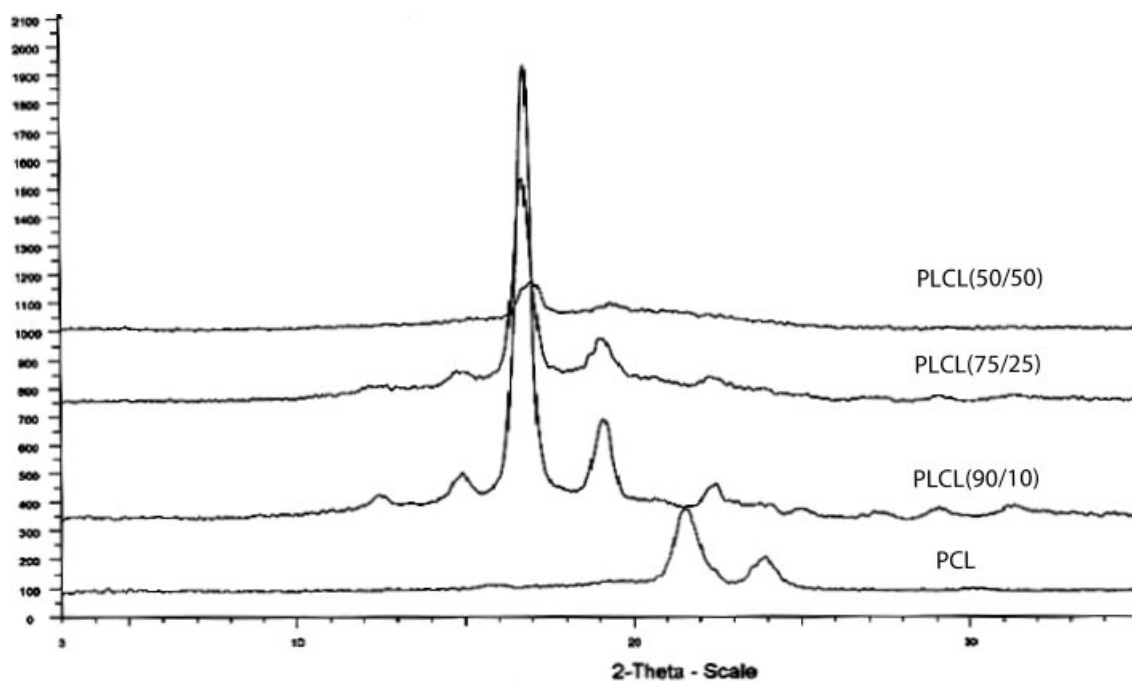


**Figure 4.** XRD spectra of the PLCL copolymers and PCL.

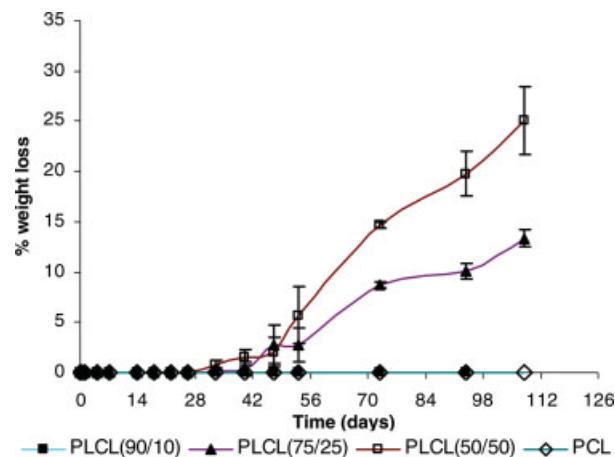


**Figure 5.** Weight loss profile of different ratios of PLCL copolymer and PCL ( $n = 4$ ). [Color figure can be viewed in the online issue, which is available at [www.interscience.wiley.com](http://www.interscience.wiley.com)]

intense peak at  $2\theta = 16.8$ , suggesting high crystallinity in all copolymers with the higher lactide ratios indicating that copolymers other than PLCL(50/50) are more crystalline. These results also support the DSC results. TGA showed weight loss in a single step with an onset of  $260\text{ }^{\circ}\text{C}$  and end-set at  $400\text{ }^{\circ}\text{C}$  suggested thermal degradation of the polymer.

### Surface Morphology of Microspheres

The microspheres were spherical with a yield of 83%–90%. Influence of copolymer type on surface morphology of microspheres could be seen in SEM results [Fig. 8(A1),(B1),(C1)]. Surface of microspheres made by PLCL (90/10) was very smooth because of its more crystalline behavior than the other copolymers. Surface of the microspheres was roughened in other copolymers and was maximum in PLCL(50/50), probably due to its amorphous nature. Porosity of the microspheres was also increased with decreasing PLA component.

### In Vitro Degradation Studies

#### Weight Loss

Weight loss of microspheres was calculated by subtracting the final weight from the initial weight of microspheres. The percentage mass loss was calculated as shown below:

% Mass loss =

$$\left( \frac{\text{Original weight} - \text{Dry weight}}{\text{Original weight}} \right) 100$$

Figure 5 shows the weight loss profiles for the copolymers used in this study. The onset and extent of weight loss was correlated to the copolymeric ratio. Weight loss started first in PLCL(50/50) ratio, followed by PLCL(75/25) and no weight loss was found in PLCL(90/10) and PCL within the degradation time of 108 days. Slow degradation of PCL was in agreement with other literature sources.<sup>2,30</sup> PLCL(50/50) and PLCL(75/25) ratio showed 1.5% and 0.37% weight loss in 40 days, respectively. Weight loss was faster in PLCL(50/50) than PLCL(75/25), possibly due to two reasons: (1) low molecular weight and (2) amorphous nature of PLCL(50/50) as compared to semicrystalline PLCL(75/25). The degradation rate is generally higher in amorphous systems than crystalline systems due to easy penetration of water front.

#### pH Change

The degradation of PLCL copolymers involves hydrolysis of ester bond, resulting in formation of lactic acid and caproic acid. Resulting decrease in pH of degradation media and acid catalysis initiated by the degradation products further results in increased degradation of polymer. pH of degradation media is thus an indicator of polymer degradation. PLCL microspheres showed a decrease in pH during the hydrolytic degradation, as expected (Fig. 6). Slow decrease in pH during initial days of degradation study was observed in all copolymers in accord with weight

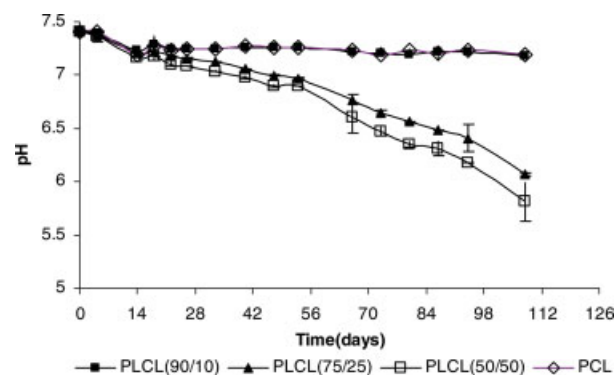


**Figure 6.** Change in pH of phosphate buffer solution during *in vitro* degradation of microspheres with different copolymer compositions at  $37\text{ }^{\circ}\text{C}$  ( $n = 4$ ). [Color figure can be viewed in the online issue, which is available at [www.interscience.wiley.com](http://www.interscience.wiley.com)]

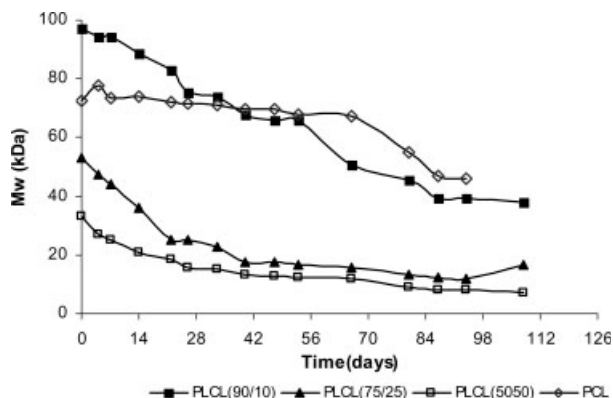


**Figure 7.** Molecular weight (Mw) change during *in vitro* degradation during *in vitro* hydrolytic degradation of microspheres of different copolymer compositions using phosphate buffer (pH 7.4) at 37 °C. GPC was used to determine the change in molecular weight of polymers.

loss. The pH of Degradation media of PLCL(90/10) and PCL microspheres were decreased insignificantly throughout degradation study, however PLCL(75/25) and PLCL(50/50) microspheres experienced faster decrease in pH after 56 days of degradation time. Highest rate of fall in pH was observed in PLCL(50/50) and was also accompanied with highest weight loss.

### Molecular Weight Change

The PLCL microspheres degraded slowly which was expected from their hydrophobic characters. Changes in molecular weights of various copolymers studied are shown in Figure 7. It was observed that copolymers of higher LA content were less crystalline than the copolymers of low LA content which facilitated good permeability for water, hence comparatively high water absorption. The other reason was that PLA chains had higher ester group content compared to PCL chains which made it more hydrophilic. Good water permeability and higher ester group content cause the copolymers of higher LA content to degrade faster in PLCL copolymer.<sup>28</sup> The study revealed that the degradation rate of copolymer was higher than its homopolymer, which was in agreement with the previous report.<sup>30</sup> PLCL(90/10) has slower degradation rate among all copolymers as it is hard and behaves more like PLLA homopolymer than as a copolymer, as observed from morphology of PLCL(90/10) microspheres (Fig. 8). This may be due to high molecular weight and high degree of microphase separation in PLCL(90/10) as melt-

ing point of copolymer was also found closer to their homopolymer.<sup>31</sup> As the LA content decreased from PLCL(90/10) to PLCL(75/25), the maximum degradation rate was seen in PLCL(75/25). Polydispersity of the copolymers was not affected during the degradation, which indicated the chain scission of low molecular weight and high molecular weight polymer at the same time in sample so that polydispersity did not follow any set pattern.

### Composition Change

A compositional change during degradation was direct indication of the polymer unit which was degraded faster. These changes were monitored by <sup>1</sup>H-NMR and observed that LA fractions of the specimens were gradually decreased with the degradation time as shown in Table 2. LA content decreased from 48 to 44.5, 74.1 to 71.7, and 91.7 to 89.6 in PLCL(50/50), PLCL(75/25) and PLCL(90/10) respectively, in 94 days which indicated LA moieties degraded faster than CL units in PLCL microspheres, due to their hydrophilicity. Lactide moiety favors the penetration of water therefore faster decrease in LA component was observed.

### Crystallinity and Thermal Property Change

The thermal property change for different ratios of PLCL during degradation is shown in Table 3. DSC thermograms illustrate the change in thermal properties of PLCL copolymer and PCL homopolymer as a function of their degradation. As already shown in Table 3, PCL homopolymer melts at 63.2 °C ( $\Delta H = 106.5$  J/g). Over the degradation of 94 days, a progressive increase in the degree of crystallinity of the PCL took place, as revealed by the shift of the melting peak 63.2 °C to 66.7 °C and increase in enthalpy along with melting peaks (106.5 J/g to 129.1 J/g). PLCL(50/50) showed two crystallizable phases of PCL and PLA having melting point at 38.8 °C ( $\Delta H = 1.9$  J/g) and 103.2 °C ( $\Delta H = 11.4$  J/g) respectively. As 100% crystalline PCL has high enthalpy ( $\Delta H = 135.6$  J/g),<sup>32</sup> an amorphous nature of PLCL(50/50) was indicated by very small enthalpy of melting, which gives degree of crystallinity as 0.014 due to PCL. Progress of degradation showed increase in crystallinity by increased melting point up to 39.1 °C and 108.6 °C for respective components.

PLA is the only component that crystallizes in PLCL(75/25), as demonstrated by the melting endotherm at 143 °C ( $\Delta H = 30$  J/g). It was only after 94 days degradation that PCL exhibited

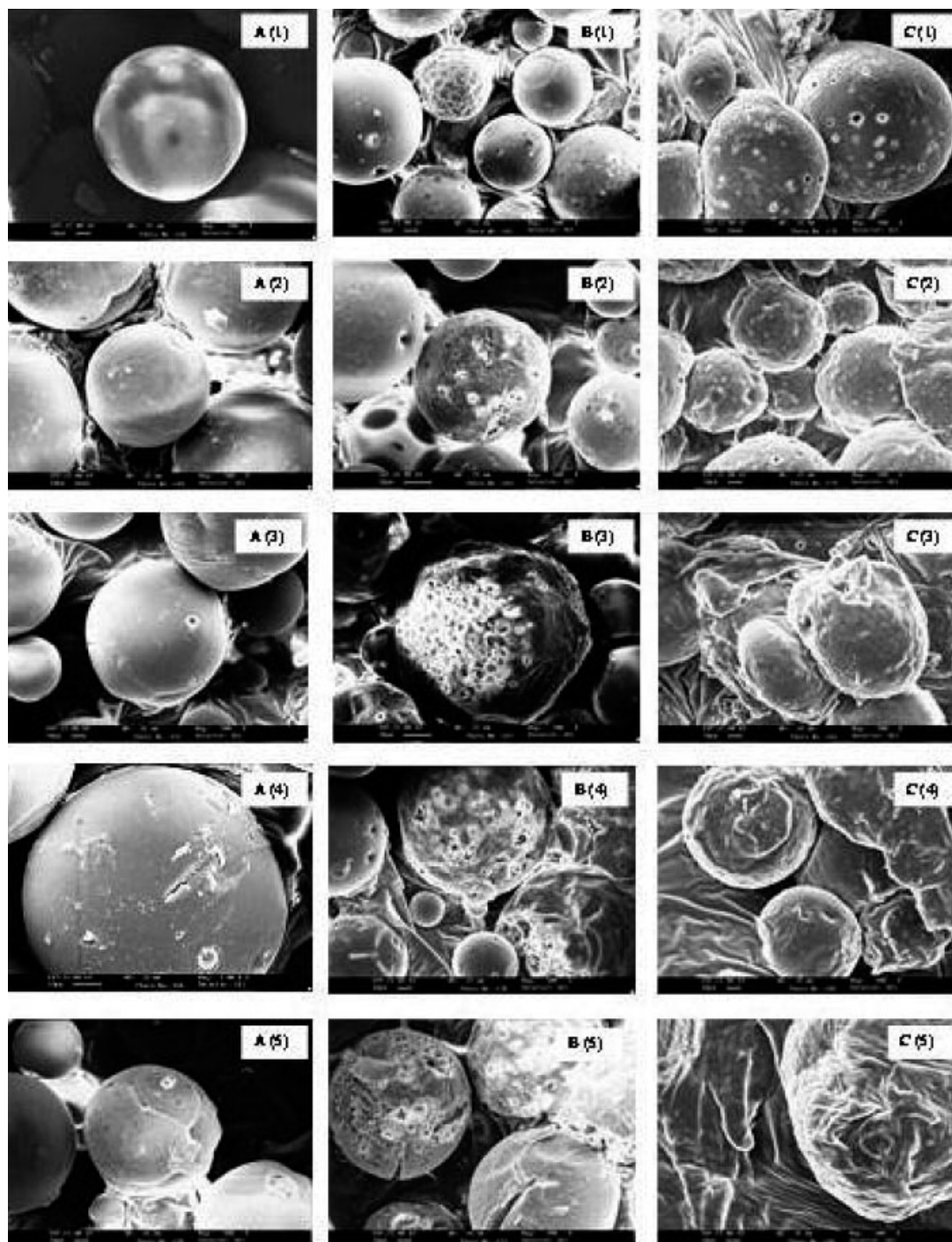


**Figure 8.** SEM photographs of PLCL microspheres showing surface morphology change during degradation PBS at pH 7.4 at 37 °C. (A) PLCL(90/10) microspheres, (B) PLCL(75/25) microspheres and (C) PLCL(50/50) microspheres at various time points 0 days (1), 33 days (2), 53 days (3), 94 days (4), and 108 days (5) for all groups of copolymers.

some degree of crystallinity, as revealed by small and broad endotherm around 39.4 °C ( $\Delta H = 24.6$  J/g). Decrease in crystallinity of PLA content during degradation was shown by a melting point

shift from 143 °C to 133.2 °C. PLCL(90/10) thermogram reveals that PCL and PLA both components melt in this copolymer ratio and over the degradation period, it was observed that a pro-

**Table 2.** Change in Polymer Composition During Hydrolytic Degradation

Degradation time (days)	Copolymers <sup>a</sup>		
	PLCL (50/50)	PLCL (75/25)	PLCL (90/10)
0	48/52	74.1/24.9	91.7/8.3
53	45.9/54.1	71.9/28.1	91.49/8.5
94	44.5/55.5	71.6/28.4	89.6/10.3

<sup>a</sup> Copolymer ratio is lactide/caprolactone; change in composition was calculated using <sup>1</sup>H NMR.

gressive increase in the degree of crystallinity of the PCL and PLA components took place during the first 53 days, as revealed by the shift of the melting peak 55.4 °C ( $\Delta H = 6.4$  J/g) to 54.7 °C ( $\Delta H = 7.9$  J/g) and 163.6 °C ( $\Delta H = 47.5$  J/g) to 164.8 °C ( $\Delta H = 55$  J/g) for the PCL and PLA component respectively, with continuous increase in enthalpy. As degradation proceeded further, at 94 days, two sharp melting endotherms at 55.2 °C ( $\Delta H = 27.5$  J/g) and 163.4 °C ( $\Delta H = 49.9$  J/g), due to the PCL and PLA segments respectively, were observed. This reveals that with further increase in time, crystallinity of PCL component increases and a decrease in PLA component crystallinity was seen because of faster degradation of PLA block in copolymer.

It is concluded from the thermal study that all the copolymers showed biphasic crystalline structure with degradation and increase in crystallinity was observed with progression of degradation time due to overall increase in PCL component. This increased PCL content was in agreement with <sup>1</sup>H-NMR results. Increase in crystallinity of microspheres along with degradation time was suggested by DSC which showed overall increase in enthalpy of copolymers.

### Morphology Change

The surface morphologies of the different types of microspheres during the degradation study were observed by scanning electron microscopy (Fig. 8). PLCL(90/10) microspheres showed a compact and smooth surface before degradation. Few oligomers are found on microspheres surface after 33 days of degradation and there was little decrease in smoothness on microsphere surface observed on 108 days of degradation period which signifies very less morphological change in PLCL(90/10) microspheres. This is in agreement with insignificant pH change and weight loss and least molecular weight reduction in PLCL(90/10), among all copolymer ratios. Degradation samples except PLCL(50/50) showed the presence of few small crystals on the microspheres surface in the area of eroding zone, which could be oligomers that are slow degrading.<sup>33</sup> PLCL(75/25) microspheres showed smooth surface with roughness and very small pores at few places, however, pore size was increased with increase in oligomers on microsphere surface after degradation of 33 days. There was further increase in pore size as degradation time increases, big holes and large cracks were seen on the 108 day of degradation study. Rough and irregular surface with big pores was seen on PLCL(50/50) microspheres. After 33 days, the number and size of the pores both decreased and some gel-like connection appeared among the pores. No pore was seen and deformation of microsphere shape was observed on 108 day, due to degradation and change of polymer property while degradation. Aforementioned differences in morphology of microspheres during degradation, were observed due to difference in physicochemical properties of polymers.

**Table 3.** Change in Thermal Properties of Copolymer Microspheres During Degradation

Polymer (LA/CL ratio)	No. of peaks	0 days		53 days		94 days	
		$\Delta H$ (J/g)	$T_m$ (°C)	$\Delta H$ (J/g)	$T_m$ (°C)	$\Delta H$ (J/g)	$T_m$ (°C)
PLCL (90/10)	2	6.4	55.4	7.9	54.7	27.5	55.2
		47.5	163.6	55.0	164.9	49.9	163.5
PLCL (75/25)	2	—	—	—	—	24.6	39.9
		30.0	143.0	15.9	134.1	20.5	133.2
PLCL (50/50)	2	1.9	38.7	5.2	39.3	3.4	39.0
		11.4	103.2	17.0	106.9	20.3	108.6
PCL	1	106.5	63.2	107.1	67.6	129.1	66.7

## CONCLUSIONS

Random copolymers of PLCL were synthesized by ROP using stannous octoate as catalyst. The properties of the copolymers changed considerably with varying compositions of copolymers. PCL is highly crystalline polymer and crystallinity of copolymer was decreased by introduction of LA block. Because of lower crystallinity and more ester groups in PLA as compared with PCL, higher water absorption was observed in copolymers with increasing LA content thus resulting in higher degradation rate of the copolymers. *In vitro* degradation behaviors suggest that hydrolytic degradation rates were also affected by LA/CL ratio and molecular weight during degradation. Effect of degradation on crystallinity studied by DSC indicates increase of crystallinity with progress of degradation time. This increase in crystallinity could be due to increase of PCL component in copolymers which was supported by <sup>1</sup>H-NMR results. Copolymers of different thermal and mechanical properties and different degradation behaviors can be obtained by adjusting the composition of copolymers. Various synthesized polymers from this work were tested in our laboratory as polymeric scaffold for soft tissue engineering.<sup>24</sup> The results have been detailed elsewhere.

K. Garkhal and S. Verma thank NIPER for their fellowships to carry out the research work. Financial support from Department of Biotechnology (DBT grant no. BT/PR7323/MED/14/979/2006) and Third World Academy of Science is duly acknowledged.

## REFERENCES AND NOTES

- Zhao, K.; Deng, Y.; Chun Chen, J.; Chen, G.-Q. *Biomaterials* 2003, 24, 1041.
- Huang, M.-H.; Li, S.; Vert, M. *Polymer* 2004, 45, 8675.
- Wu, L.; Ding, J. *Biomaterials* 2004, 25, 5821.
- Ciardelli, G.; Chiono, V.; Vozzi, G.; Pracella, M.; Ahluwalia, A.; Barbani, N.; Cristallini, C.; Giusti, P. *Biomacromolecules* 2005, 6, 1961.
- Cui, Y.; Zhao, X.; Tang, X.; Luo, Y. *Biomaterials* 2004, 25, 451.
- Huang, M.; Li, S.; Coudane, J.; Vert, M. *Macromol Chem Phys* 2003, 204, 1994.
- Li, Y.; Zhu, K. J.; Zhang, J. X.; Jiang, H. L.; Liu, J. H.; Hao, Y. L.; Yasuda, H.; Ichimaru, A.; Yamamoto, K. *Int J Pharm* 2005, 295, 67.
- Williamsa, J. M.; Adewunmib, A.; Scheka, R. M.; Flanagan, C. L.; Krebsbach, P. H.; Feinbergd, S. E.; Hollistera, S. J.; Dasb, S. *Biomaterials* 2005, 26, 4817.
- Kikuchi, M.; Koyama, Y.; Yamada, T.; Imamura, Y.; Okada, T.; Shirahama, N.; Akita, K.; Takakuda, K.; Tanaka, J. *Biomaterials* 2004, 25, 5979.
- Lee, S.; Kim, B.; Kim, S. H.; Choi, S. W.; Jeong, S. I.; Kwon, I. K.; Kang, S. W.; Nikolovski, J.; Mooney, D. J.; Han, Y.; Kim, Y. H. *J Biomed Mater Res A* 2003, 66, 29.
- Jeong, S. I.; Kwon, J. H.; Lim, J. I.; Cho, S. W.; Jung, Y.; Sung, W. J.; Kim, S. H.; Kim, Y. H.; Lee, Y. M.; Kim, B. S.; Choi, C. Y.; Kim, S. J. *Biomaterials* 2005, 26, 1405.
- Yang, X.; Zhao, K.; Chen, G. *Biomaterials* 2002, 23, 1391.
- Kwon, I. K.; Kidoaki, S.; Matsuda, T. *Biomaterials* 2005, 26, 3929.
- Cooper, J. A.; Lu, H. H.; Ko, F. K.; Freeman, J. W.; Laurencin, C. T. *Biomaterials* 2005, 26, 1523.
- Park, H.; Temenoff, J. S.; Holland, T. A.; Tabata, Y.; Mikosa, A. G. *Biomaterials* 2005, 26, 7095.
- Holland, T. A.; Tabata, Y.; Mikos, A. G. *J Control Release* 2005, 101, 111.
- Nguyen, H.; Qian, J. J.; Bhatnagar, R. S.; Li, S. *Biochem Biophys Res Commun* 2003, 311, 179.
- Mercier, N. R.; Costantino, H. R.; Tracy, M. A.; Bonassar, L. J. *Biomaterials* 2005, 26, 1945.
- Huang, M.-H.; Coudane, J.; Li, S.; Vert, M. *J Polym Sci Part A: Polym Chem* 2005, 43, 4196.
- Teng, C.; Yang, K.; Ji, P.; Yu, M. *J Polym Sci Part A: Polym Chem* 2004, 42, 5045.
- Jeong, S. I.; Kim, B. S.; Lee, Y. M.; Ihn, K. J.; Kim, S. H.; Kim, Y. H. *Biomacromolecules* 2004, 5, 1303.
- Zhu, Y.; Chian, K. S.; Chan-Park, M. B.; Mhaisalkar, P. S.; Ratner, B. D. *Biomaterials* 2006, 27, 68.
- Gunatillake, P. A.; Adhikari, R. *Eur Cell Mater* 2003, 5, 1.
- Garkhal, K.; Verma, S.; Tikoo, K.; Kumar, N. *J Biomed Mater Res A*, 80A: 2007 (In press).
- Sahoo, S. K.; Panda, A. K.; Labhasetwar, V. *Biomacromolecules* 2005, 6, 1132.
- Jeong, S. I.; Kim, B.-S.; Kang, S. W.; Kwon, J. H.; Lee, Y. M.; Kim, S. H.; Kim, Y. H. *Biomaterials* 2004, 25, 5939.
- Maglio, G.; Migliozi, A.; Palumbo, R. *Polymer* 2003, 44, 369.
- Qian, H.; Bei, J.; Wang, S. *Polym Degrad Stabil* 2000, 68, 423.
- Cohn, D.; Salomon, A. H. *Biomaterials* 2005, 26, 2297.
- Ye, W. P.; Du, F. S.; Jin, W. H.; Yang, J. Y.; Xu, Y. *React Funct Polym* 1997, 32, 161.
- Wang, M.; Zhang, L.; Ma, D. *Eur Polym J* 1999, 35, 1335.
- Lefevre, C.; Villers, D.; Koch, M. H. J.; David, C. *Polymer* 2001, 42, 8769.
- Modi, S.; Jain, J. P.; Kumar, N. *Isr J Chem* 2005, 45, 401.